Journal of Physics B: Atomic, Molecular and Optical Physics

PAPER • **OPEN ACCESS**

Investigation of buffer gas trapping of positrons

To cite this article: C J Baker *et al* 2020 *J. Phys. B: At. Mol. Opt. Phys.* **53** 185201

OPEN ACCESS
IOP Publishing
Journal of Physics B: Atomic, Molecular and Optical Physics
J. Phys. B: At. Mol. Opt. Phys. **53** (2020) 185201 (7pp)
https://doi.org/10.1088/1361-6455/aba10c

Investigation of buffer gas trapping of positrons

C J Baker[1], C A Isaac, D Edwards[2], H T Evans, R Clayton, D P van der Werf and M Charlton

Department of Physics, College of Science, Swansea University, Singleton Park, Swansea, SA2 8PP, United Kingdom

E-mail: c.baker@swansea.ac.uk

Received 2 April 2020, revised 5 June 2020
Accepted for publication 29 June 2020
Published 22 July 2020

Abstract

A study of positron capture in a two-(pressure) stage buffer gas accumulation apparatus is presented for a variety of species, including some molecules which are known to be either efficient for positron trapping, or are frequently used to cool the particles when held in these devices. Absolute accumulation efficiencies are reported for all species. A detailed optimisation procedure, which has identified the main processes responsible for positron capture and loss in the trap, has been deployed to explore accumulation efficiency as the gas pressure and the electrostatic well depth in the trap are systematically varied. Accumulation exploiting energy loss via molecular vibrational transitions has been observed for the first time for a number of gases, though at much lower efficiency than achieved using electronic excitation processes.

Keywords: positron, buffer gas accumulation, scattering

(Some figures may appear in colour only in the online journal)

1. Introduction

The positron (e^+), the antimatter counterpart of the electron (e^-), has been probed and employed for a variety of studies, ranging from materials engineering to antihydrogen production. While some types of investigation are possible utilising positrons directly from β^+-emitting isotopes, such as copper-64 and sodium-22, major breakthroughs have been forthcoming since the arrival of the first low-energy e^+ beams [1]. There has been much improvement of the devices producing the beams, up to the current systems that are capable of providing fluxes of around 10^6–10^7 s^{-1} (radionuclide, laboratory-based beams: see, e.g. [2, 3]) and 10^9–10^{10} s^{-1} (large facility-based beams: see e.g. [4]). Despite this, instantaneous e^+ fluxes are still low, and as such many experiments have benefitted greatly from, or indeed been made possible by, the development of the buffer gas trap (BGT), or accumulator (see e.g. Danielson *et al* [5]), which has enabled large numbers of positrons to become available in ns-wide pulses to advance experimentation with, for instance, positronium (Ps, the e^+–e^- bound state: see, e.g. [6] and references therein), the positronium molecule (Ps_2, [7, 8]) and the formation and trapping of, and experimentation with, antihydrogen ($\bar{H}$, [9–23]).

Most of the BGT systems currently in use rely upon a sodium-22-based, rare gas solid-moderated [24, 25], e^+ beam, with trapping accomplished by kinetic energy loss via excitation of the $a^1\Pi$ electronic transition in molecular nitrogen gas, resulting in confinement in a Penning–Malmberg trap (an arrangement of hollow cylindrical electrodes, appropriately electrically biased, immersed in a solenoidal magnetic field; see section 2) as developed by Surko and co-workers [26, 27]. Such devices have a maximum accumulation efficiency of $\sim$30% although 10%–20% is more typical due to competing optimisations dictated by experimental requirements.

The advances facilitated by the use of the BGT have led naturally to the proposal of alternative accumulation schemes,

[1] Author to whom any correspondence should be addressed.
[2] Present address: Laser Physics Centre, Research School of Physics and Engineering, Australian National University, 60 Mills Road, Acton, ACT 2601, Australia

such as the use of an electron cloud to promote energy loss [28] or the use of buffer gases other than molecular nitrogen (e.g. [29]). It is the latter which is of interest here, and in particular the work of Marjanović *et al* [29], who studied the use of the $\nu 3$ vibrational excitation mode in carbon tetraflouride (CF_4) due to its comparatively high cross section and open scattering channel at e^+ kinetic energies below the threshold for the positron loss process of Ps formation[3]. An attempt to demonstrate e^+ accumulation using CF_4 as the buffer gas proved to be unsuccessful [30], with elastic backscattering of the e^+ beam on the molecules in the higher magnetic field of the BGT (when compared to the field during transport to the trap) cited as the likely limitation.

Typical positron-atom (A) and -molecule (XY) scattering processes at the incident kinetic energies used in BGTs are as follows:

$$e^+ + \mathrm{A/XY} \rightarrow e^+ + \mathrm{A/XY}: \quad \text{elastic scattering}, \tag{1}$$

$$e^+ + \mathrm{A/XY} \rightarrow 2\gamma + \mathrm{A^+/XY^+}: \quad \text{annihilation in flight}, \tag{2}$$

$$e^+ + \mathrm{A/XY} \rightarrow \mathrm{Ps} + \mathrm{A^+/XY^+}: \text{direct positronium formation}, \tag{3}$$

$$e^+ + \mathrm{A/XY} \rightarrow e^{+'} + \mathrm{A^*/XY^*}: \quad \text{atomic/molecular excitation, and} \tag{4}$$

$$e^+ + \mathrm{A/XY} \rightarrow e^{+'} + e^- + \mathrm{A^+/XY^+}: \quad \text{direct ionisation}. \tag{5}$$

Here $e^{+'}$ denotes a positron which has lost kinetic energy via transfer to atomic or molecular excitation ($\mathrm{A^*/XY^*}$), with the electronic and (for molecules at lower trapped e^+ kinetic energies) vibrational channels of main concern here, or via ionisation of the molecule ($\mathrm{A^+/XY^+}$). Furthermore, for some molecules, processes involving fragmentation (e.g. $e^+ + \mathrm{XY} \rightarrow \mathrm{Ps} + \mathrm{X^+} + \mathrm{Y}$ and $e^+ + \mathrm{XY} \rightarrow e^{+'} + e^- + \mathrm{X^+} + \mathrm{Y}$) are important/dominant contributors to energy loss [31, 32].

Positron trapping is typically facilitated via energy loss from excitation and ionisation processes (reactions 4 and 5, and also, in some instances, the aforementioned fragmentation reactions) during passage through the BGT, with the main loss channel being that due to Ps formation (reaction 3). The relative cross sections for these processes, and their energy-dependence, are crucial in determining the trapping efficiency, along with experimental parameters, such as the trap pressure and length, and the voltages applied to the trap electrodes. Elastic scattering (reaction 1) can redistribute e^+ kinetic energy between the axial and transverse directions (see the discussion in section 3) whilst the lifetime in the trap is determined by annihilation (process 2) and cross field transport [33].

Herein we report accumulation of positrons for a number of molecular species, and for argon gas, using excitation/ionisation as the energy loss process (with lower efficiency, though of comparable order of magnitude, than for the ubiquitous N_2 buffer gas). We discuss these data in terms of the various beam and BGT parameters, together with the relevant scattering processes which promote or prevent trapping. Separately, we investigate accumulation using molecular vibrational excitation (and in particular the $\nu 3$ mode of CF_4) which we have found to be an order of magnitude less efficient. Section 2 contains a brief discussion of the BGT used for the study, whilst section 3 describes positron beam properties and aspects of scattering of relevance for e^+ trapping. Our accumulation results are presented in section 4 and we conclude with section 5.

2. Apparatus

There are two generic types of BGT currently in use: the original three-(pressure) stage system [27], typically applied when very large (say $\sim 10^8$) e^+ numbers are the primary requirement (see e.g. [11]); and the more compact two-stage device, such as that used in the present study, and employed at higher repetition rates, with a commensurately lower positron number in each cycle [2, 3, 34, 35].

Though the construction and operation of the Swansea positron two-stage system, shown schematically in figure 1, has been described extensively elsewhere [3, 33], details relevant to the present study will be discussed here. The positron source, an iThemba Labs sealed sodium-22 β^+ emitter, is inserted into a tungsten–copper alloy capsule holder, into which a cartridge-type heating element is installed and a chromel-Fe thermocouple attached. The capsule holder is thermally connected, but electrically isolated by a 20 mm outer diameter, 3 mm thick sapphire disk, to a Sumitomo RDK408 cold head which cools the source assembly to $\sim$5.7 K (as reported by the aforementioned thermocouple). The source capsule is secured into its holder using a copper cone arrangement which is screwed over the source and onto the holder. This assembly contains a truncated and inverted, 15.7° half angle, cone of length 15 mm, such that the smaller opening has a diameter of 5 mm (to match the diameter of the source emission window) and a larger opening diameter of 10 mm to allow the moderated positrons to form a beam. The electrical isolation of the capsule, holder and cone allows an accelerating potential, V_s, of 85.0 V to be applied. The cold head condenses 99.999% pure neon gas onto the cryogenic surfaces, resulting in a low energy e^+ beam, produced with an efficiency of $\sim$0.5% of the source activity. The gas is admitted into the vacuum chamber, of base pressure $<10^{-9}$ mbar as measured by a cold cathode ionisation gauge, for 30–40 min while a PID controlled piezoelectric valve maintains a constant system pressure of $\leqslant 10^{-2}$ mbar as measured by a Pirani gauge. This part of the beamline is immersed within an axial magnetic field B_s of $\sim$8 mT, which provides the required radial confinement of the beam.

The low energy e^+ emitted from the condensed Ne are then magnetically guided approximately 2 m downstream by a series of quasi-Helmholtz coils and a transport solenoid until they reach the trap electrodes. These are contained within a $B_t = 35$ mT solenoid which provides radial confinement

[3] Positron loss via direct, in-flight, annihilation (reaction 2) although possible at all kinetic energies, has a cross section several orders of magnitude lower than those for other scattering processes.

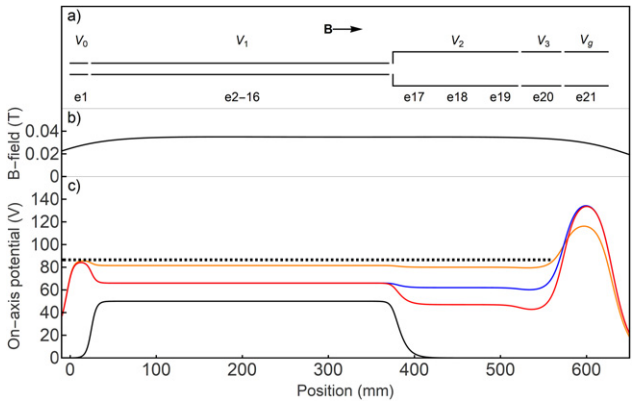

Figure 1. (a) Sketch of the electrode configuration with electrode numbers and voltage regions V_0, V_1, V_2, V_3 and V_g highlighted (see text for details). (b) On-axis magnetic field. (c) The on-axis electrical potential for two trapping schemes based on electronic excitation of CF_4 (red & blue lines), an example trap configuration when trapping using vibrational excitation (orange line), and an example V_1 retarding potential analyser configuration (black line). A typical moderated e^+ beam energy is indicated by the dashed band at ∼86 eV.

for the e^+ in the BGT: see figure 1(b). Axial confinement is achieved by applying appropriate electrical potentials to the 21 hollow cylindrical electrodes which make up the trap: see figures 1(a) and (c). The first, high pressure, stage of the trap is comprised of 16 gold-plated aluminium cylinders of inner diameter 16 mm, outer diameter 20 mm and of length 24 mm, with shaped ends such that when assembled with 1 mm diameter sapphire spheres (to provide mutual electrical insulation) there is no direct line of sight from outside the assembly to the inner surfaces. This first stage is electrically configured such that the 1st electrode encountered by the incoming positron beam can be independently biased, whilst electrodes 2 to 16 are coupled by an external potential divider circuit. The remaining five independently bias-able electrodes are also gold-plated aluminium cylinders of larger diameter, with inner and outer diameters of 41 mm and 50 mm, respectively, and with a length of 49 mm with similarly shaped ends. It should be noted that electrode 20 is halved lengthwise, with one half azimuthally segmented into four identical parts to facilitate the application of a so-called rotating wall, though for the study presented in sections 3 and 4 it was electrically connected such that all parts were at the same voltage. All electrical biases are provided by custom-built amplifiers based around a PA341 op-amp with typical 90%–10% fall times of 10 μs and 10 mV RMS noise. The electrically isolated nature of electrodes 2–16 can be utilised to produce a potential gradient across the first stage (and not a constant V_1) but no significant change in the accumulation rate was observed for fields up to ∼200 mV cm^{-1} in this study.

To facilitate e^+ accumulation, the gas under study is admitted into the system through a small, 2 mm diameter, hole in electrode 10 (approximately located at the middle of the first stage) with a PID controlled piezoelectric valve, stabilised on one of a number of cold cathode ionisation, or capacitance, gauges as required. A 400 ls^{-1} turbo pump approximately 20 cm upstream of the entrance electrode (e1), a 800 ls^{-1} cryogenic storage pump approximately 20 cm downstream of the exit electrode (e21), the various electrode inner diameters, and the piezoelectric valve combine to produce a static, but scalable, pressure profile within the trap.

Positrons are trapped continuously, and once the desired accumulation is complete, the cycle is terminated by ejection of the e^+ cloud in a 10–20 ns wide bunch. Positron detection is accomplished destructively by directing them towards a grounded stainless steel plate at the exit of the trap and registering the resulting annihilation gamma-ray flash using a 1 cm^3 CsI(Tl) crystal coupled to an avalanche photodiode. The diode output is read and recorded by a PC-based digitiser configured to measure the integrated gamma signal coincident with e^+ ejection from the trap when the electrical potential applied to electrode 21 is removed. The same detector can also monitor the count rate of the moderated, unbunched, e^+ beam by counting the number of individual gammas that exceed a preset electrical noise threshold. This was used to monitor the beam during retarding potential analyser, RPA, measurements (see section 3), and in a normalisation procedure [3, 36] which has allowed the absolute accumulation/trapping efficiency to be extracted, and such data will be discussed in section 4.

3. Positron beam and scattering

Although the initial positron kinetic energy is largely set by V_s applied to the source assembly, the positrons are emitted epithermally from the solid neon moderator surface. While the resulting energy distribution has been studied for a freshly deposited (presumably clean) moderator and is understood in terms of energy loss mechanisms and their thresholds [24], it is observed that the distribution changes over time, probably via contamination by the buffer gas which inevitably condenses onto the cryogenic surfaces. This deposition not only affects the moderator yield, but can cause a shift in the energies of the emitted positrons. The low energy positron flux is typically depressed and the modified kinetic energy may change the accumulation efficiency.

By applying suitable voltages to various electrodes within the trap, it may be employed as an RPA in which the DC count rate on the annihilation target can be monitored as the electrode bias V_i is varied—either to the first or second stage of the trap, V_1 and V_2, respectively. Electrodes are grounded when not in use, as illustrated in figure 1(c). Figure 2(a) shows examples of typical RPA curves for the normalised positron count rate N, and the data without gas (which is indicative of the positron beam parallel kinetic energy distribution) has been fitted [37] using

$$N = C + A\,\mathrm{Erf}\left(\frac{eV_i - E_{\parallel}^{\mathrm{t}}}{\sqrt{2}E_{\sigma}^{\mathrm{t}}}\right), \qquad (6)$$

with A and C constants, and e the elementary charge. This has allowed estimates of the mean positron energy parallel to the magnetic field in the trap, $E_{\parallel}^{\mathrm{t}}$, and the parallel energy spread E_{σ}^{t} to be determined. For a freshly deposited moderator, as depicted in figure 2(a), the typical values are $E_{\parallel}^{\mathrm{t}} = 86.6 \pm 0.1$ eV and $E_{\sigma}^{\mathrm{t}} = 2.3 \pm 0.1$ eV, for the magnetic fields B_s and B_t

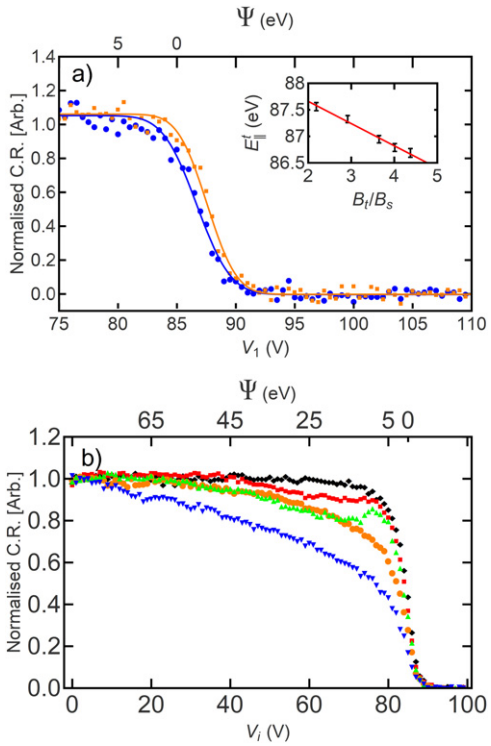

Figure 2. (a) Positron count rate (C.R.) data taken using the RPA method (normalised to unity for full beam transmission) for a freshly deposited neon moderator, with no gas present in the trap and magnetic fields $B_t = 17.5$ mT (▪) and 35 mT (▪), within the buffer gas trap. The fits using equation (6) assume a Gaussian parallel energy distribution [37]. Inset: $E^t_\parallel$ for various B_t (at a constant B_s) with the linear fit using equation (7) providing the mean total positron energy as 88.5 ± 0.1 eV and $E^s_\perp = 0.42 \pm 0.02$ eV. (b) RPA data for no gas and varying V_2 (•), nitrogen gas and varying V_1 (▪) and V_2 (•), and CF_4 gas and varying V_1 (▲) and V_2 (▼). The gas pressures were identical in each case and estimated to be 2×10^{-3} mbar in the first stage of the trap.

given in section 2. This model assumes a Gaussian energy distribution for the emitted positrons that is unmodified (other than the change in $E_\parallel$ and E_σ) due to the adiabatic invariant involving the perpendicular energy $E_\perp$ as $\mu = E_\perp/B$ by the varying magnitude of the magnetic fields along the beam transport system. This assumption is valid as the maximum adiabacity parameter [38] in our system is 0.1 near the entrance to the transport solenoid. Using the 'magnetic beach' technique [39, 40] the total positron energy E can be determined using the conservation of (kinetic) energy and the invariance of μ as,

$$E^t_\parallel = E - E^s_\perp \frac{B_t}{B_s} \tag{7}$$

with $E^s_\perp$ the perpendicular energy in the source region, and an example of data obeying this relationship is shown in the inset of figure 2(a). For reference $\Psi = e(V_s - V_i)$ has been included as a guide to $E^t_\parallel$.

In addition to such RPA measurements, studies have been performed in order to allude positron interactions with the buffer gas without the complications of trapping. In one such study for nitrogen gas (red squares in figure 2(b)) V_1 was biased in the presence of the buffer gas and the transmitted count rate monitored. Although significantly broadened by the relatively large energy spread of the beam, the onset of an energy dependent loss mechanism can be observed at $\Psi \sim (eV_s - 45) \approx 40$ eV, which continues to $\Psi \sim (eV_s - 75) \approx 10$ eV and we suggest this is due to positronium formation via reaction 3 (which has a threshold at around 9 eV), following comparison with cross sections collected by Petrović *et al* [41], where the cross section for Ps formation peaks at $2–3 \times 10^{-16}$ cm^2 at around 20 eV (with a corresponding collisional mean free path of ∼0.7–1 m). In a separate study (orange circles figure 2(b)), the second stage voltage V_2 was varied in order to investigate the positron parallel energy distribution after interaction with the entire column of the buffer gas. In this case, the continuous loss of positron counts and apparent larger E^t_σ, stretching across almost the entire applied voltage span, appear consistent with reaction 1, elastic scattering of positrons passing through the higher pressure 1st stage, either reducing the parallel energy being probed and/or energy losses due to reactions 4 and 5, the excitation and ionisation of the nitrogen molecules. The mean free paths of these processes are in the range 0.7–2.5 m.

Similar measurements were performed on CF_4, by varying V_1 (green up-triangles in figure 2(b)) which show a very similar (to N_2) continuous loss for $\Psi \gtrsim (eV_s - 45) \approx 40$ eV which is probably caused by elastic scattering (which has a cross section $>6 \times 10^{-16}$ cm^2, and mean free path of <0.3 m), before a further decrease in the transmitted yield between $\Psi \lesssim (eV_s - 45) \approx 40$ eV and $\Psi \gtrsim (eV_s - 75) \approx 10$ eV which we suggest is due to Ps formation and ionisation, including fragmentation (cross sections $>2 \times 10^{-16}$ cm^2 and up to 3×10^{-16} cm^2 respectively, or mean free paths of 0.7–1 m). This conclusion is supported by the increase in count rate between $\Psi \lesssim (eV_s - 75) \approx 10$ eV and $\Psi \gtrsim (eV_s - 80) \approx 5$ eV whereupon both the Ps formation and CF_4 electronic excitation and ionisation channels effectively turn off, leaving elastic scattering and the $\nu 3$ vibrational excitation channel (with a mean free path of ∼0.4 m) as the primary parallel energy loss mechanisms. Varying V_2 with CF_4 present (blue down-triangles in figure 2(b)) results in a significantly larger decrease in count rate across all energies due to all the various channels available. Similar behaviour is also seen in other gases, such as SF_6.

4. Positron accumulation

In order to fully, and in an automated fashion, scan the trapping conditions, a Monte Carlo approach was employed to investigate the optimum potentials to apply to the trap electrodes. Operating in a clear (all potentials set to ground), accumulate for time t_a, and eject cycle, the electrode potentials were randomly selected subject to the following conditions:

$$V_s = 85 \text{ V},$$
$$V_s \geqslant V_0 \geqslant V_s - 5 \text{ V},$$
$$V_{i-1} \geqslant V_i \geqslant V_{i-1} - 20 \text{ V} \quad \text{and}$$
$$V_g = 140 \text{ V},$$

where $i = 1, 2, 3$ such that, specifically and with reference to figure 1(a), V_0 is the potential applied to electrode 1, V_1 is

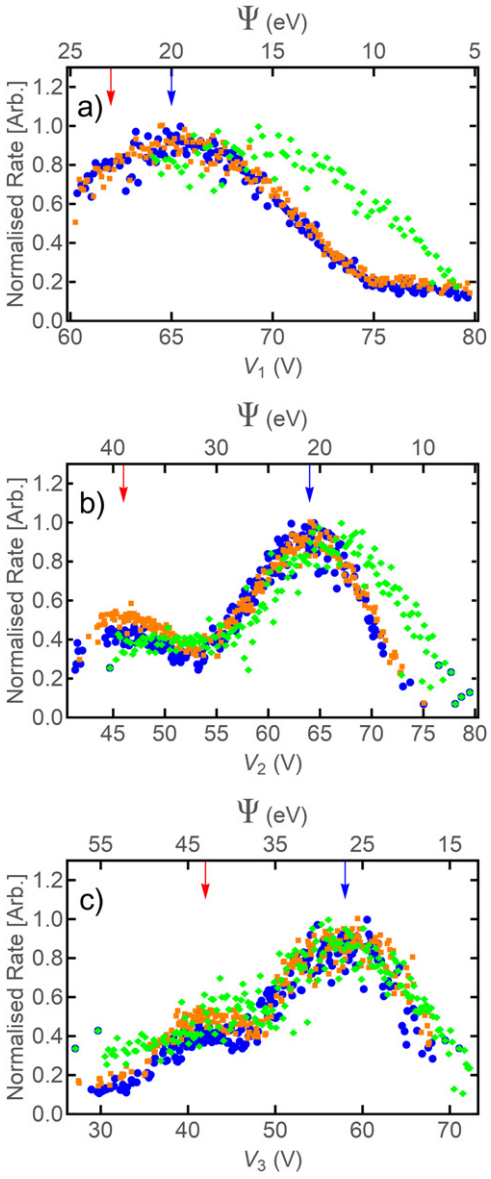

Figure 3. Accumulation of positrons using various electrode potentials on CF_4 for gas pressures in the first stage of the trap of 7×10^{-4} mbar (•), 4.5×10^{-4} mbar (▪) and SF_6 for 1.4×10^{-3} mbar (•). A guide to the kinetic energy of the positrons in the various trap stages is given along the top axes as the parameter Ψ (see section 3). The panels (a)–(c) show the results of varying the voltage (and therefore the trap depth) in stages 1, 2 and 3 respectively across different ranges. The red and blue arrows indicate the example accumulator voltages of each stage as illustrated in figure 1(c).

applied to electrodes 2–16 which form the 1st trapping stage, V_2 is applied to electrodes 17–19, with V_3 applied to electrode 20, and V_g is the final confining potential (note, $V_g > V_s$ in order to repel the low energy positrons that did not lose sufficient parallel energy when they initially traversed the 1st and 2nd stages).

With a chosen set of potentials applied to the electrodes, t_a was varied and the resulting captured positron number, N_e, recorded in order to produce a so-called accumulation curve. From this the accumulation rate, R, is extracted by fitting the data with

$$N_e(t_a) = N(\infty)\left(1 - \exp\left[-\frac{t_a}{\tau}\right]\right) = R\tau\left(1 - \exp\left[-\frac{t_a}{\tau}\right]\right), \quad (8)$$

where τ is the lifetime of the positrons within the trap.

In order to correct for the moderator changes discussed in section 3 a 'standard' accumulation cycle (which can vary from gas to gas, but is chosen to have a high accumulated e^+ yield) with fixed experimental parameters, was regularly interleaved with the experimental runs and used for a simple numerical normalisation.

The accumulation rates (normalised to the standard cycle) from the equation (8) fit for potentials applied to the trap electrodes are presented in figure 3. Comparing the regions of high accumulation rates with the e^+–CF_4 cross section data it appears that the positron is electronically exciting the CF_4 molecule and accumulation proceeds via a process similar to that of nitrogen: electronic excitation and ionisation occur within the 1st stage and further energy losses occur within the 2nd stage via other mechanisms (blue arrows), or at lower pressures electronic excitation occurs within the 1st stage and further electronic excitation(s) occur within the 2nd stage (red arrows). Note that the blue and red arrows correspond to the blue and red trapping configurations depicted in figure 1(c).

Given the beam data, and that the maximum $\nu 3$ vibrational excitation cross section is higher than those for the electronic processes and is finite at energies where several particle loss channels are unavailable, it is reasonable to postulate, as was done by Marjanović *et al* [29], that significantly increased accumulation rates are possible. To probe this a similar approach was employed to investigate low energy accumulation (i.e. the accumulation conditions were modified such that $V_3 \leqslant V_s - 4$ V, with an appropriate voltage hierarchy maintained across the stages). Although accumulation curves were obtained (confirming the ability to capture e^+ using the $\nu 3$ vibrational excitation channel of CF_4), within the experimental uncertainties no distinct structure similar to that of figure 3 was found. We attribute this to the broad energy spread of the incoming positron beam.

By varying the flow rate of gas into the accumulator the behaviour of the accumulation rate with respect to pressure could be obtained and is presented in figure 4 (normalised to the low energy positron beam flux to provide an overall efficiency) for various buffer gases[4]. It is notable that identical

[4] There is, however, some uncertainty regarding the absolute gas pressures at the entrance to the accumulator, and more importantly the pressures within the 1st stage. For the former, the relevant calibration for the cold cathode gauge is unavailable and the relative ionisation efficiencies for the gases are unknown. Nevertheless, for pressures below 10^{-5} mbar, capacitance gauges within the apparatus gas feed lines are available for cross calibration and report <1% variation between simultaneous measurements of the gas under study. Given the close correlation between these gauges, and the ionisation gauge, the linear response of the ionisation gauge and the similar ionisation energies for the various gases, the pressure comparison of figure 4 is reasonable. To establish absolute pressures in the 1st stage, the primary concern is gas flow and effective pumping speeds over the orders of magnitude change in pressure explored. This could be addressed using detailed finite element modelling, but it is not envisaged that such a simulation would add meaningfully to the present study (it could only change the pressure required for the maximum accumulation rate, not the observed rate) or improve the accuracy of the pressures beyond a factor of ∼2.

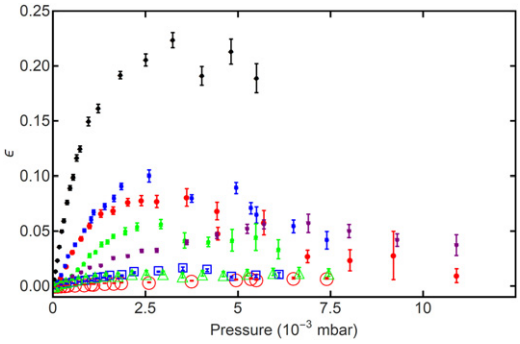

Figure 4. Accumulation efficiency ($\epsilon = R$/beam intensity) with respect to the pressure within the first stage of the trap for N_2 (•), SF_6 (•○), CF_4 (■□), CO_2 (▲△), and Ar (▼) using trapping schemes to promote electronic (solids) and vibrational (hollow) energy loss mechanisms.

potentials were used for several different gases yet, as suggested by the SF_6 data presented in figure 3, the highest accumulation rates (and hence efficiencies) do not occur at identical values of V_i. However, multiple trials at various pressures have revealed no higher accumulation rate, presumably since E_σ^t is comparable to the broad range of V_is (Ψ) where the maximum accumulation rate occurs.

Our finding that N_2 is the most efficient buffer gas is consistent with previous work. The capture of e^+ using energy loss via electronic excitation involves a competition between that process and loss via Ps formation: reactions 4 and 3, respectively. The cross section for the latter typically rises rapidly from threshold (see, e.g. [42–44]) and dominates that for excitation, which for atomic and most simple molecular species has an energy threshold in excess of that for the formation of Ps [45, 46]. However, uniquely, not only does N_2 possess an excitation threshold slightly lower than that for Ps formation, but the cross section for population of the $a^1\Pi$ states rises steeply to a resonance-like feature after a few eV [43, 47]. As pointed out in [43], and illustrated further in [30], this is the reason for the higher efficiency for N_2 when compared to other species. We note that taking a simple estimate of the fraction of the e^+ interacting in the accumulator, as described in section 3 we find a capture efficiency of around 40% for N_2 which, given the aforementioned uncertainty in the absolute gas density, is in reasonable accord with the measured overall efficiency[5].

Accumulation at low e^+ energies, as illustrated in the efficiency plot in figure 4, has been attributed to the excitation of vibrational modes. Of the molecules we have investigated, CF_4, CO_2 and N_2 have low energy vibrational cross section data available [41, 48–50]. Making a similar estimate of efficiency to that described above for capture by electronic excitation of N_2 we find values of around 5% for both CF_4 and CO_2 and more than two orders of magnitude lower for N_2. In particular, the latter is in accord with our failure to observe a trapped e^+ signal for N_2 at low energies. This also suggests that accumulation via large angle elastic scattering is inefficient, though a fully quantitative comparison of the various targets would require differential scattering cross sections for all species, many of which, as emphasised elsewhere [41], are not available. To further support our contention that vibrational excitation is responsible for accumulation at low energies we note that under the low energy trap conditions the very small overlap of the high energy tail of the positron beam distribution with the relevant electronic channels implies capture efficiencies well below 0.1% from these processes.

Fitting equation (8) to the obtained accumulation curves also allows the lifetime of positrons within the trap to be ascertained. While the uncertainty in these values is somewhat large due to the choice of t_a (selected to more accurately obtain the accumulation rate), those obtained have revealed that τ is, as expected, inversely proportional to the gas pressure, but for CF_4, for example, commensurate with the lifetime obtained from artificially scaling the nitrogen lifetimes by the ratio of elastic cross sections between nitrogen and CF_4. Thus, it is suggested that the dominant loss mechanism is collisional, cross field, radial transport of the positrons to the electrode walls, rather than direct annihilation (reaction 2). Indeed expansion rates of e^+s accumulated using CF_4 have been measured for various pressures and appear consistent with those obtained previously [51], while the contribution from reaction 2 is similar for all gases investigated as the products of the relevant annihilation parameter, the effective number of e^-s per atom/molecule available to the e^+ for annihilation, $Z_{\rm eff}$ [45, 52], and the gas pressures used are broadly comparable.

5. Concluding remarks

The study presented here has demonstrated the accumulation of positrons using several molecular gases, and argon, and compared their efficiencies with respect to nitrogen as the current industry standard. In particular, we have successfully accumulated positrons using CF_4, SF_6, and CO_2 using both electronic and vibrational energy loss channels with the former providing efficiencies similar to those for N_2, with the latter roughly at one-tenth. We propose that the latter effect is due to the broad energy spread of the solid neon moderated e^+ beam (see section 3) employed for this study, and the low energy loss per e^+–molecule interaction. As well as the backscattering effect noted by Marjanović *et al* [30], their failure to observe any accumulation using the vibrational excitation of CF_4 may also be due to an injudicious choice of accumulator potential profile. (The current study was also unsuccessful in observing evidence for e^+ accumulation using such a shallow potential profile, i.e. $V_3 \leqslant V_0 - 2$ V, while limiting e^+ backscatter by reducing B_t to $\sim B_s$ did not yield a higher accumulation efficiency, presumably because E_σ^t is still comparatively large.)

The observation that cross field transport is the dominant loss mechanism in the accumulator for all gases suggests that it can be mitigated by the application of the so called 'rotating wall' technique (as has been employed for the nitrogen buffer gas [11]). While a detailed study is yet

[5] The e^+ path length in the accumulator and the estimated mean free paths can provide a guide to the number of $e^+ + XY$ collisions within the first stage of the apparatus. By considering the e^+ beam energy distribution in the trap the probability of collision can be derived to give an estimate of the capture efficiency.

to be performed, increased e^+ lifetimes, and commensurately increased e^+ number, have been observed. However, despite this observation, as concluded by Marjanović *et al* [30], the CF_4 vibrational energy loss mechanism is not expected to exceed the typical nitrogen scheme with the existing hardware. Although the electronic energy loss mechanism could prove to be comparable, which may lead to a possible system simplification by the removal of one gas (CF_4 is often employed at low pressures as a second cooling gas when the rotating wall technique is engaged), such future apparatus would likely require a different pressure profile (and hence electrode size/configuration).

Acknowledgments

The authors would like to thank the EPSRC (UK, Award EP/P024734/1) for funding the antimatter research at Swansea. We are grateful to previous group members, and for the enthusiastic support given to us by the College of Science technical team.

ORCID iDs

C J Baker https://orcid.org/0000-0002-9448-8419
C A Isaac https://orcid.org/0000-0002-7813-1903
D Edwards https://orcid.org/0000-0003-1255-6367
H T Evans https://orcid.org/0000-0001-6745-4187
D P van der Werf https://orcid.org/0000-0001-5436-5214
M Charlton https://orcid.org/0000-0002-9754-1932

References

[1] Canter K F, Coleman P G, Griffith T C and Heyland G R 1972 *J. Phys. B: At. Mol. Phys.* **5** L167
[2] Cassidy D B, Deng S H M, Greaves R G and Mills A P Jr 2006 *Rev. Sci. Instrum.* **77** 073106
[3] Clarke J, van der Werf D P, Griffiths B, Beddows D C S, Charlton M, Telle H H and Watkeys P R 2006 *Rev. Sci. Instrum.* **77** 063302
[4] Hugenschmidt C *et al* 2014 *J. Phys.: Conf. Ser.* **505** 012029
[5] Danielson J R, Dubin D H E, Greaves R G and Surko C M 2015 *Rev. Mod. Phys.* **87** 247
[6] Cassidy D B 2018 *Eur. J. Phys.* D **72** 53
[7] Cassidy D B and Mills A P Jr 2007 *Nature* **449** 195
[8] Cassidy D B, Hisakado T H, Tom H W K and Mills A P Jr 2012 *Phys. Rev. Lett.* **108** 133402
[9] Amoretti M *et al* (ATHENA Collaboration) 2002 *Nature* **419** 456
[10] Gabrielse G *et al* (ATRAP Collaboration) 2002 *Phys. Rev. Lett.* **89** 213401
[11] Jørgensen L V *et al* (ATHENA Collaboration) 2005 *Phys. Rev. Lett.* **95** 025002
[12] Andresen G B *et al* (ALPHA Collaboration) 2010 *Nature* **468** 673
[13] Andresen G B *et al* (ALPHA Collaboration) 2011 *Nat. Phys.* **7** 558
[14] Gabrielse G *et al* (ATRAP Collaboration) 2012 *Phys. Rev. Lett.* **108** 113002
[15] Ahmadi M *et al* (ALPHA Collaboration) 2017 *Nat. Commun.* **8** 681
[16] Amole C *et al* (ALPHA Collaboration) 2012 *Nature* **483** 439
[17] Amole C *et al* (ALPHA Collaboration) 2013 *Nat. Commun.* **4** 1785
[18] Ahmadi M *et al* (ALPHA Collaboration) 2017 *Nature* **548** 66
[19] Amole C *et al* (ALPHA Collaboration) 2014 *Nat. Commun.* **5** 3955
[20] Ahmadi M *et al* (ALPHA Collaboration) 2016 *Nature* **529** 373
[21] Ahmadi M *et al* (ALPHA Collaboration) 2017 *Nature* **541** 506
[22] Ahmadi M *et al* (ALPHA Collaboration) 2018 *Nature* **561** 211
[23] Ahmadi M *et al* (ALPHA Collaboration) 2020 *Nature* **578** 375
[24] Mills A P Jr and Gullikson E M 1986 *Appl. Phys. Lett.* **49** 1121
[25] Khatri R, Charlton M, Sferlazzo P, Lynn K G, Mills A P Jr and Roellig L O 1990 *Appl. Phys. Lett.* **57** 2374
[26] Surko C M, Leventhal M and Passner A 1989 *Phys. Rev. Lett.* **62** 901
[27] Murphy T J and Surko C M 1992 *Phys. Rev.* A **46** 5696
[28] Oshima N, Kojima T M, Nigaki M, Mohri A, Komaki K and Yamazaki Y 2004 *Phys. Rev. Lett.* **93** 195001
[29] Marjanović S, Šuvakov M, Banković A, Savić M, Malović G, Buckman S J and Petrović Z 2011 *IEEE Trans. Plasma Sci.* **39** 2614
[30] Marjanović S, Banković A, Cassidy D B, Cooper B, Deller A, Dujko S and Petrović Z L 2016 *J. Phys. B: At. Mol. Opt. Phys.* **49** 215001
[31] Moxom J, Schrader D M, Laricchia G, Xu J and Hulett L D 2000 *Phys. Rev.* A **62** 052708
[32] Christophorou L G and Olthoff J K 2002 *Appl. Surf. Sci.* **192** 309
[33] van der Werf D P, Isaac C A, Baker C J, Mortensen T, Kerrigan S J and Charlton M 2012 *New J. Phys.* **14** 075022
[34] Sullivan J P, Jones A, Caradonna P, Makochekanwa C and Buckman S J 2008 *Rev. Sci. Instrum.* **79** 113105
[35] Cooper B S, Alonso A M, Deller A, Wall T E and Cassidy D B 2015 *Rev. Sci. Instrum.* **86** 103101
[36] Amoretti M *et al* (ATHENA Collaboration) 2004 *Nucl. Instrum. Methods Phys. Res.* A **518** 679
[37] Natisin M R, Danielson J R and Surko C M 2015 *Phys. Plasmas* **22** 033501
[38] Ghosh S, Danielson J R and Surko C M 2020 *J. Phys. B: At. Mol. Opt. Phys.* **53** 085701
[39] Hsu T and Hirschfield J L 1976 *Rev. Sci. Instrum.* **47** 236
[40] Hyatt A W, Driscoll C F and Malmberg J H 1987 *Phys. Rev. Lett.* **26** 2975
[41] Petrović Z L *et al* 2013 *AIP Conf. Proc.* **1545** 115
[42] Marler J P, Sullivan J P and Surko C M 2005 *Phys. Rev.* A **71** 022701
[43] Marler J P and Surko C M 2005 *Phys. Rev.* A **72** 062713
[44] Laricchia G, Armitage S, Kövér A and Murtagh D J 2008 *Adv. At. Mol. Opt. Phys.* **56** 1
[45] Charlton M 1985 *Rep. Prog. Phys.* **48** 737
[46] Schrader D M and Svetic R E 1982 *Can. J. Phys.* **60** 517
[47] Sullivan J P, Marler J P, Gilbert S J, Buckman S J and Surko C M 2001 *Phys. Rev. Lett.* **87** 073201
[48] Gilbert S J, Greaves R G and Surko C M 1999 *Phys. Rev. Lett.* **82** 5032
[49] Sullivan J P, Gilbert S J and Surko C M 2001 *Phys. Rev. Lett.* **86** 1494
[50] Marler J P and Surko C M 2005 *Phys. Rev.* A **72** 062702
[51] Mortensen T 2013 Manipulation of the magnetron orbits of particles and clouds in a two-stage buffer gas accumulator *PhD Thesis* Swansea University
[52] Iwata K, Greaves R G, Murphy T J, Tinkle M D and Surko C M 1995 *Phys. Rev.* A **51** 473